Available online at www.sciencedirect.com
ScienceDirect
Building and Environment 42 (2007) 3161–3165
BUILDING AND ENVIRONMENT
www.elsevier.com/locate/buildenv

Influence of zeolite additive on properties of autoclaved aerated concrete

Mustafa Albayrak[a,*], Abdulkerim Yörükoğlu[a], Serdar Karahan[a], Sema Atlıhan[a], H. Yılmaz Aruntaş[b], İsmail Girgin[c]

[a]*Mineral Research and Exploration General Directorate, 06520 Ankara, Turkey*
[b]*Faculty of Technical Education, Department of Construction, Gazi University, 06500 Ankara, Turkey*
[c]*Mining Engineering Department, Hacettepe University, 06532 Beytepe, Ankara, Turkey*

Received 26 January 2006; received in revised form 4 July 2006; accepted 22 August 2006

Abstract

In this experimental study, the effect of zeolite on the properties of autoclaved aerated concrete (AAC) was investigated. Zeolite was used as a quartzite replacement in conventional AAC mixtures. The zeolite containing AAC (ZAAC) specimens were prepared at bulk densities of 270–500 kg/m^3. The specimens were examined by X-ray diffraction, X-ray fluorescence, and thermal analysis. Bulk density, compressive strength and thermal conductivity parameters were investigated. According to the results of research, the commercial AAC is mainly composed of tobermorite, quartz and anhydrite, but the specimens of ZAAC, besides tobermorite and quartz, contain unreacted anhydrite and clinoptilolite phases. XRD patterns of ZAAC obtained after treatment at 700–1000 °C show that wollastonite, gehlenite and orthoclase are the new phases formed. It was observed that application of zeolite in AAC significantly lowered the thermal conductivity of autoclaved products (0.08–0.12 kcal/m h °C) providing the compressive strength at the level of 1.22−3.34 N/mm^2.
© 2006 Elsevier Ltd. All rights reserved.

Keywords: Autoclaved aerated concrete; Thermal treatment; Zeolite; X-ray diffraction; Compressive strength; Thermal conductivity

1. Introduction

Autoclaved aerated concrete (AAC) is produced using cement, lime, siliceous materials (quartz sand, fly ash) and small quantities of aluminum powder [1]. These components are mixed with water, molded and transferred to a porous mass by generation of a hydrogen gas at atmospheric pressure. The aluminum powder acts as a gas-forming agent. Following the reaction time of several hours, soft and workable mass is obtained due to the hydration of unslaked lime and cement. Then, the shaped material is cured for nearly 10 h at 180–190 °C using saturated steam at pressure of around 12 bar. The final products have an average compressive strength of 2.5–7.5 MPa and a oven-dry unit weight of 400–600 kg/m^3 depending on the quality class (G2–G6 according to TS 453).

With steam curing, an initially formed C–S–H phase is transferred to tobermorite ($5CaO\ 6SiO_2 \cdot 5H_2O$) by reaction with dissolved silica with excess quartz remaining unreacted. It has been reported that the hydrothermal reactions in the $CaO–SiO_2$ system are controlled by the dissolution of quartz [2–5], which is the dominating factor for the processing time. Isu et al. [6] studied the effect of quartz particle size and found that the crystallinity of tobermorite was increased with increase of quartz particle size. Gyrolite ($Ca_4(Si_6O_{15})(OH)_2 \cdot 3H_2O$) was formed with an increased autoclaving time in case when finer quartz was used. Isu et al. [7] showed that the formation of gyrolite after reaction time of 64 h using finer quartz decreased the compressive strength and the Young's modulus due to changes in the micro-pore size distribution.

Hauser et al. [8] used fly ash from cellulose industries in AAC mixtures and observed that, at a high proportion of fly ash, the formation of calcium silicate hydrate phases was delayed with corresponding drop in strength and increase in shrinkage. Wägner et al. [9] found that the anisotropy in AAC could be precisely monitored by

*Corresponding author. Tel.: +90 312 2873430.
E-mail address: albayrakalbayrak@gmail.com (M. Albayrak).

0360-1323/$ - see front matter © 2006 Elsevier Ltd. All rights reserved.
doi:10.1016/j.buildenv.2006.08.003

measurement of gas permeability rather than determining the compressive strength values, especially for lower-density products. Other researchers have studied the compressive strength and drying shrinkage of AAC [10–12].

The aim of this work was to investigate the effect of zeolite as siliceous material replacing quartz sand in AAC. For this purpose, the effect of Manisa-Gördes clinoptilolite (Turkey) on chemical and mechanical properties of ZAAC was examined.

2. Experimental study

2.1. Materials

Zeolite used in this study was obtained from Gördes Zeolite Works (Turkey). The specific gravity of the sample was determined as 2.28 and the chemical composition of the sample is given in Table 1. The chemical composition of conventional siliceous material used in AAC composition is given Table 1 [13]. The XRD analysis of zeolite sample shows that the main mineral is clinoptilolite and cristobalite is present in minor quantities.

XRD patterns of the sample treated at temperatures between 100 and 800 °C (Fig. 1) show that the peak intensities of clinoptilolite are decreased due to lattice contraction and thermal collapse of the framework at 800 °C. The TG/DTA data given in Fig. 2 is in agreement with XRD results showing continuous dehydration up to 700 °C with the release of water and an exothermic event at 924.2 °C due to collapse of the structure. At temperatures between 900 °C and 1300 °C color changes are observed and new phases are formed (Fig. 3). Yellowish pale brown color at 1150 °C (opal-CT, quartz and feldspars) turns into gray at 1300 °C with the observed phase of quartz.

2.2. Sample preparation

Based on the proportions of the raw mixtures [5,6,11] ZAAC samples were prepared at varying bulk densities with mean ratio of $Ca/(Al+Si) = 0.48$. In all these samples zeolite with size of less than 90 μm was used to replace quartz at a dosage of 100%. The samples were cast using $300 \times 200 \times 200$ mm steel molds, initially hardened at atmospheric pressure and temperature of around 50 °C for 4 h and then autoclaved at 200 °C under saturated steam pressure of 11.5 bar for 12 h using the facilities of Çimentaş AAC factory.

2.3. Methods of investigation

Compressive strength and bulk density were determined in accordance with TS 453 "Gas and foam concrete

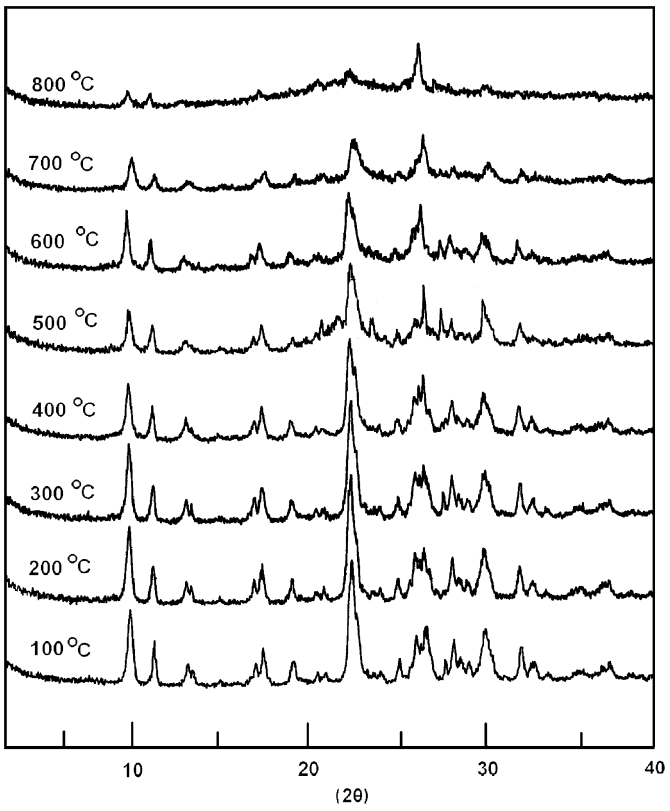

Fig. 1. XRD patterns of zeolite between 100 and 800 °C.

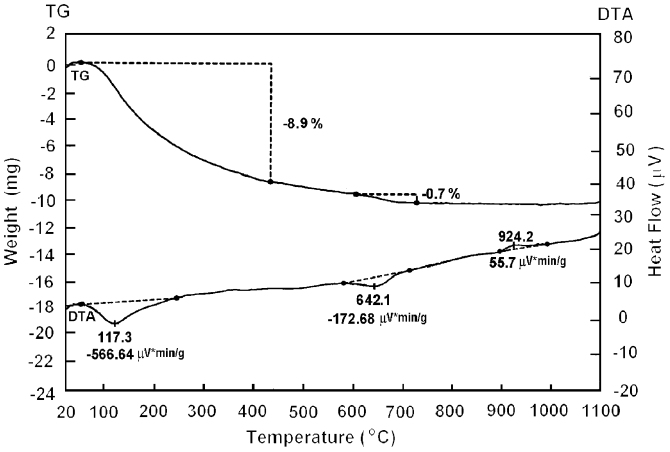

Fig. 2. TG/DTA curves of zeolite.

Table 1
Chemical composition of the zeolite (clinoptilolite) and quartzite

Oxide	SiO_2	Al_2O_3	K_2O	CaO	Fe_2O_3	MgO	Na_2O	TiO_2	L.O.I.
Zeolite	70.74	12.77	3.59	2.21	1.30	1.16	0.53	0.023	7.55
Quartzite	97.58	0.31	0.03	0.14	1.20	0.10	0.10	—	0.03

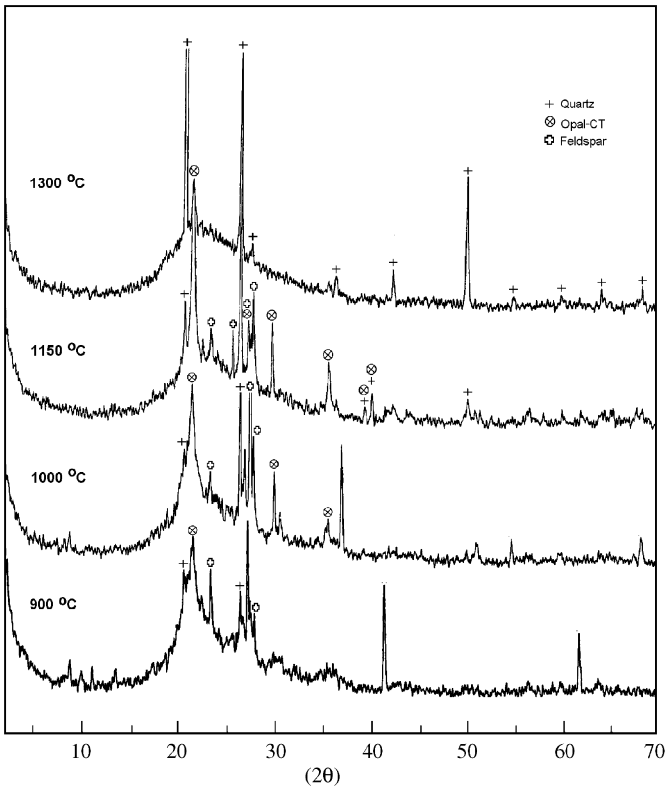

Fig. 3. XRD patterns of zeolite after treatment at 900–1300 °C.

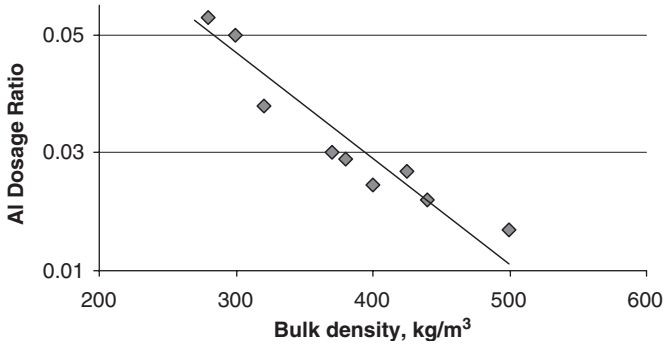

Fig. 4. Change of dry bulk density of ZAAC with the ratio of Al/∑Al.

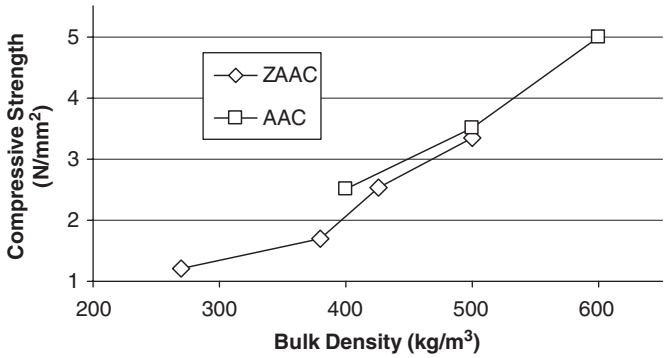

Fig. 5. Compressive strength of investigated concrete vs. dry bulk density.

material and elements for buildings" [14]. Compressive strength tests were performed on 100 mm cubic specimens at the age of 28 days. The loading rate was arranged to achieve the failure in 30 s by keeping the stress rate between 0.05 and 0.25 N/mm^2. Bulk density was determined on $150 \times 100 \times 40$ mm samples dried at 105 ± 5 °C. Thermal conductivity measurements were done in accordance with TS ISO 8302 "Thermal insulation: determination of steady-state thermal resistance and related properties; guarded hot plate apparatus"[15] using Kemtherm QTM-D3 thermal conductivity meter on dry samples.

Chemical composition of zeolite was determined by X-ray fluorescence analysis using Rigaku RIX 3000 spectrometer. X-ray diffraction (XRD) analyze was carried out on a Rigaku Geiger Flex X-ray diffractometer and the TG/DTA tests were performed using Rigaku TAS 100 Thermoflex TG 8110 thermal analyzer.

3. Results and discussion

3.1. Bulk density, compressive strength and thermal conductivity

Zeolite-based AAC (ZAAC) samples were prepared at the oven-dry unit weight of 270–500 kg/m^3 by controlling the quantity of Al used as foaming agent. Change of ZAAC bulk density at different Al/∑Al ratio is given in Fig. 4, showing that the bulk density increases sharply with decrease of Al powder dosage.

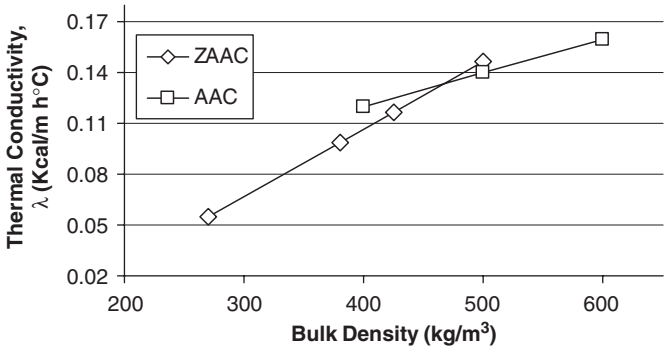

Fig. 6. Thermal conductivity of investigated concrete vs. dry bulk density.

Changes in compressive strength and thermal conductivity values vs. dry bulk density of ZAAC and commercial AAC are given in Figs. 5 and 6 (as per as TS 453 and TS 415 EN 12939 [14,16]). The compressive strength and the thermal conductivity values are reduced with decrease of bulk density of these materials. Similar thermal conductivity values were observed for ZAAC and AAC products of the same density.

3.2. X-ray diffraction and thermal analysis of products

XRD analyses (Fig. 7) show the presence of tobermorite, quartz and anhydrite in commercial AAC and formation of wollastonite as a new phase at 850 °C. Typical TG/DTA curve of commercial G-2 grade AAC is given in Fig. 8. Two

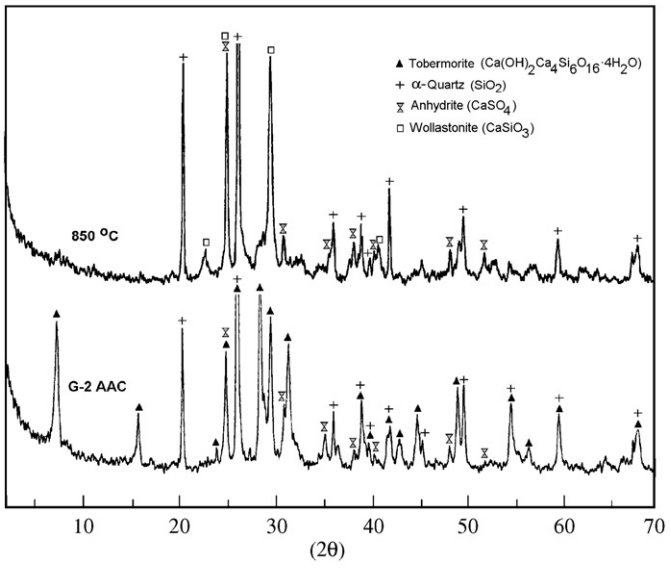

Fig. 7. XRD pattern of G-2 grade AAC at 25 °C and 850 °C.

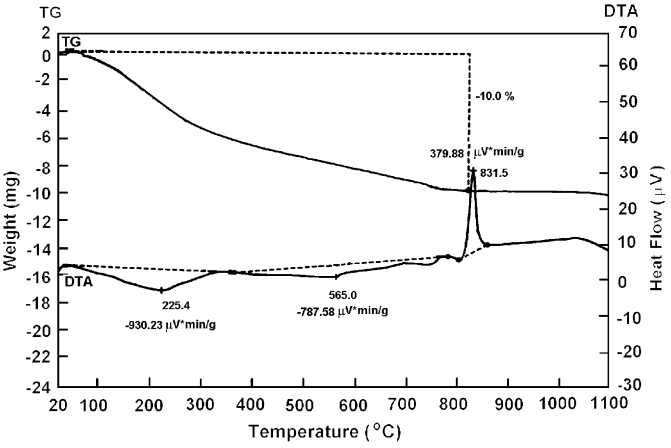

Fig. 8. TG/ DTA curve of commercial G-2 grade AAC.

endotherms observed for AAC at 225.4 °C and at 565.0 °C are due to loss of molecular water and conversion of α-SiO_2 to β-SiO_2, respectively. The sharp exotherm at 831.5 °C is associated with crystallization of wollastonite.

The ZAAC contain unreacted anhydrite and clinoptilolite phases besides tobermorite and quartz (Fig. 9). XRD patterns obtained after treatment of the product between 700 and 1000 °C show that wollastonite, gehlenite and orthoclase are newly formed phases. Clinoptilolite (zeolite) peaks were also observed at 700–800 °C in sample. While gehlenite was observed at temperature 800–1000 °C, wollastonite and orthoclase were observed only at 900–1000 °C. On the other hand, there was no detected change with anhydrite phase. Initially formed tobermorite disappeared with increase in temperature.

DTA curve for ZAAC (Fig. 10) shows that an endotherm occurring at 161.7 °C is due to loss of molecular water; two exotherms at 755.0 and 798.5 °C are due to lattice contraction and thermal collapse of the framework of excess clinoptilolite and a broad exotherm at 877.1 °C

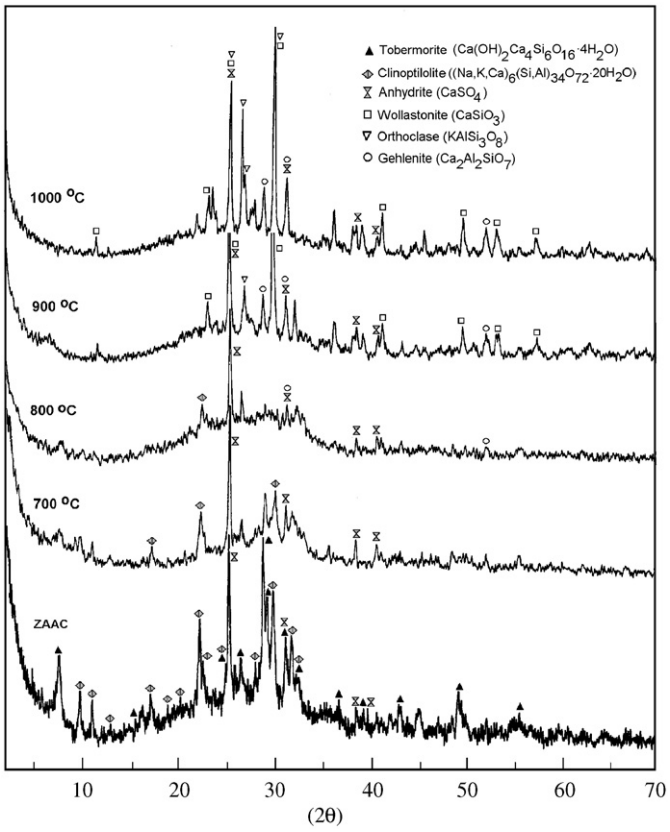

Fig. 9. XRD patterns of ZAAC at 25 °C and 700–1000 °C.

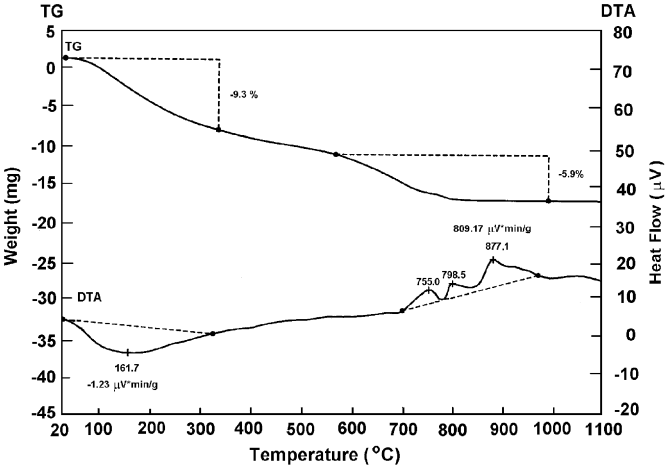

Fig. 10. TG/DTA curves of ZAAC.

can be attributed to formation of wollastonite as a new phase.

4. Conclusions

The following conclusions can be made based on the results of this investigation:

1. Zeolite can be used as a component of AAC partially replacing quartzite and providing the strength similar to

conventional AAC. With increase in the bulk density of ZAAC and AAC the compressive strength of these materials increases proportionally.

2. Use of zeolite to replace quartzite in production of AAC provides the thermal conductivity values similar to conventional AAC at the same bulk density.
3. Commercial AAC is mainly composed of tobermorite, quartz and anhydrite, but ZAAC contains unreacted anhydrite and clinoptilolite phases besides tobermorite and quartz.
4. XRD patterns obtained after treatment of ZAAC between 700 and 1000 °C shows that wollastonite, gehlenite and orthoclase are the new phases formed at these temperatures.

References

[1] Guide for precast cellular concrete—floor, roof, and wall units ACI 523.2R-96. American Concrete Institute, Cellular Concrete Committee 523, 1996.
[2] Kondo R. Autoclaved calcium silicate building products. London, England: Society of Chemical Industry; 1967.
[3] El-Hemaly SAS, Mitsuda T, Taylor HFW. Synthesis of normal and anomalous tobermorites. Cem Concr Res 1977;7:429–38.
[4] Chan CF, Mitsuda T. Formation of 11 Å tobermorite from mixture of lime and colloidal silica with quartz. Cem Concr Res 1978;8:135–8.
[5] Mitsuda T, Sasaki K, Ishida H. Phase evolution during autoclaving process of aerated concrete. J Am Ceram Soc 1992;75(7):1858–63.
[6] Isu N, Ishida H, Mitsuda T. Influence of quartz particle size on the chemical and mechanical properties of autoclaved aerated concrete (I) tobermorite formation. Cem Concr Res 1995;25(2): 243–8.
[7] Isu N, Teramura S, Ishida H, Mitsuda T. Influence of quartz particle size on the chemical and mechanical properties of autoclaved aerated concrete (II) fracture toughness, strength and micropore. Cem Concr Res 1995;25(2):249–54.
[8] Hauser A, Eggenberger U, Mumenthaler T. Fly ash from cellulose industry as secondary raw material in autoclaved aerated concrete. Cem Concr Res 1999;29(3):297–302.
[9] Wägner F, Schober G, Mörtel H. Measurement of the gas permeability of autoclaved aerated concrete in conjunction with its physical properties. Cem Concr Res 1995;25(8):1621–6.
[10] Alexanderson J. Relations between structure and mechanical properties of autoclaved aerated concrete. Cem Concr Res 1979;9: 507–14.
[11] Georgiades A, Ftikos AG, Marinos J. Effect of micropore structure on autoclaved aerated concrete shrinkage. Cem Concr Res 1991;21:655–62.
[12] Narayanan N. Microstructural investigations on aerated concrete. Cem Concr Res 2000;30(3):457–64.
[13] Pettijohn FJ. Sedimentary rocks. New York: Harper & Row Publishers; 1975 (p. 233).
[14] TS 453. Gas and foam concrete material and elements for building. Ankara: Turkish Standards Institution; 1988.
[15] TS ISO 8302. Thermal insulation; determination of steady-state thermal resistance and related properties; guarded hot plate apparatus. Ankara: Turkish Standards Institution; 2002.
[16] TS 415 EN 12939. Thermal performance of building materials and products—determination of thermal resistance by means of guarded hot plate and heat flow meter methods. Ankara: Turkish Standards Institution; 2005.